

RESEARCH PAPER

Application of near-infrared light intensity to determine normal and cancerous breast vessel contrast by gold nanoparticles

Parinaz Mehmati ¹, Bahman Alipour ^{2*}, Roya Salehi ³

¹Department of Medical Physics, School of Medicine, Tabriz University of Medical Sciences, Tabriz, Iran

²Medical Radiation Sciences Research Team, Tabriz University of Medical Sciences, Tabriz, Iran

³Drug Applied Research Center, Tabriz University of Medical Sciences, Tabriz, Iran

ABSTRACT

Objective(s): A novel technique for the early diagnosis of breast cancer involves the use of nanoparticles (NPs). The present study aimed to use gold NPs to assess the variations in light source transfer intensity.

Materials and Methods: Blood samples with hemoglobin (Hb) concentrations of $\times 1$, $\times 2$, and $\times 4$ were used to simulate normal and cancerous conditions in the breast. Spherical gold NPs (SGNPs) and gold nanorods (GNRs) with various Hb concentrations were injected into the breast phantom, and the intensity of the light transmitted on the wavelength of 635 nanometers was measured. Transmission electron microscopy (TEM) images revealed that SGNPs and GNRs were prepared with a uniform particle shape.

Results: When the SGNPs were blended with the Hb concentrations of $\times 1$, $\times 2$, and $\times 4$, the intensity of the passing light from the vessel was estimated to be 3.62, 2.40, and 1.64 mw, respectively. When GNRs were blended with the Hb concentrations of $\times 1$, $\times 2$, and $\times 4$, the intensity changed to lower values 3.42, 2.13, and 1.98 mw, respectively.

Conclusion: According to the results, SGNPs and GNRs in normal and cancerous breast induced various passing intensities of Hb concentrations. In addition, the vascular contrast induced by GNRs was higher compared to SGNPs.

Keywords: Breast cancer, Hemoglobin, Rod-shaped gold nanoparticles Spherical gold nanoparticles, Simulation

How to cite this article

Mehmati P, Alipour B, Salehi R. Application of near-infrared light intensity to determine normal and cancerous breast vessel contrast by gold nanoparticles. *Nanomed J.* 2019; 6(3):207-213. DOI: 10.22038/nmj.2019.06.00007

INTRODUCTION

Breast cancer is a widespread cancer in women, which is only second to skin cancer. It could be developed in both men and women although the incidence is rather unusual in men. Breast cancer is associated with a high mortality rate among women each year [1]. Evidently, the early diagnosis and treatment of breast cancer could reduce the mortality rate by 95% in patients [2].

Various methods are available for the diagnosis of breast tumors, such as magnetic resonance imaging (MRI), ultrasound (US), computed tomography (CT), conventional mammography, and optical mammography, each of which has its own limitations. CT and mammography involve the use of ionizing radiation and have limited resolution [3, 4]. Moreover, the sensitivity of some of these systems is a function of age. For

instance, mammography has reached its highest sensitivity in the women aged 50 years and is not recommended for those aged less than 40 years [5].

Use of light in optical mammography, especially if the source is near-infrared (NIR), has non-ionizing properties, low costs, and the ability to show the variations in the hemoglobin (Hb) concentration. Therefore, it could be inferred that using methods with high accuracy and reliability for the early detection of breast cancer remains a significant challenge in medicine.

Tumor tissues could absorb nutrients and oxygen through transpiration up to the distance of 70-150 micrometers [6]. Tumor growth necessitates the tumor to develop a new vascular network. Consequently, tumor detection in the vascularization stage should be as early as possible in order to be able to control the tumor growth and even to treat it [7].

It has been well established that tumor tissues have elevated Hb content compared to normal

* Corresponding Author Email: bahmanalipour69@gmail.com

Note. This manuscript was submitted on December 10, 2018; approved on April 5, 2019

tissues [8, 9]. Hb concentrations are directly associated with the number of blood vessels (angiogenesis) and play a key role in tumor cell growth [10]. According to the literature, the mean Hb concentration in normal women is $34 \pm 9 \mu\text{mol/l}$ in pre-menopausal cases and $14 \pm 0 \mu\text{mol/l}$ in post-menopausal cases [10, 11]. In a systematic review, Leff *et al.* reported that breast cancer patients have a mean Hb concentration of approximately $65 \pm 34 \mu\text{mol/l}$, which is almost twice higher than the women with normal breasts ($\text{Hb} = 21 \pm 6 \mu\text{mol/l}$). This shows a difference of two and four times between the Hb concentrations in normal and abnormal cases, explaining the reason for the use of $\times 1$ Hb as normal tissues, as well as $\times 2$ and $\times 4$ Hb as abnormal breast tissues. This cause-and-effect relationship could be applicable in the identification and differentiation of healthy and unhealthy breast cells. Use of nanoparticles in various Hb concentrations is associated with benefits such as high permeability, fast-tracking of nanoparticles, and sensing and imaging enhancement, which result in better conditions for the detection of the changes in the Hb concentrations of normal cells. Therefore, the present study could be an effective step toward the early detection of breast cancer.

In the current research, spherical and rod-shaped gold nanoparticles were used. Gold nanoparticles (GNPs) have been widely investigated owing to their unique physical and optical properties, which arise from their surface plasmon resonance (SPR) properties. SPR is associated with the combined excitation of conduction electrons, which is localized in a broad spectrum from the visible to the infrared (IR) region depending on the particle size, shape, and structure [12, 13]. SPR is the resonant oscillation of conduction electrons at the interface between the negative and positive permittivity material stimulated by the incident light [14, 15].

With SPR, GNPs have exceptionally high absorption coefficients, which allow higher sensitivity in optical detection methods compared to conventional organic dyes, making them viable candidates for the development of biomarker platforms [14]. GNPs have numerous advantages in biomedical applications, including the ease of addition to functional biomolecules, high efficiency in penetrating cells, and ability to respond to light at near-infrared wavelengths [16]. Since the optical properties of gold NPs depend

on their shape, SPR could be easily tuned to offer the maximum absorption of 500 nanometers to the near-infrared point in the spectrum [17]. As a result, we used gold NPs in two shapes in order to examine their induced vascular contrast in breast phantom vessels. The difference in the absorption properties of the SGNPs and GNRs of the same average size is due to the anisotropic distribution of the surface electron layers [18].

Rod-shaped SGNPs trigger higher signals in surface-enhanced Raman spectroscopy (SERS) due to the enhancement of the electromagnetic field on the surface, which is caused by irregular-shaped particles [14]. In the present study, near-infrared light was used to determine the variations in light intensity at various concentrations of Hb since near-infrared has a non-invasive, higher signal-to-background ratio and is safe in repeating the non-ionizing method, while it could also penetrate the depths of tissues more effectively compared to optical lights [19].

Previous studies have indicated good separation in various concentrations of Hb at the wavelengths of 620-640 nanometers with absorption characteristics [20]. For instance, Taroni *et al.* proposed the contrast of tumor tissues with the diameter of 1.5 centimeters to 637 nanometers [21, 22].

The present study aimed to evaluate the variations in the transmission intensity of near-infrared light at various concentrations of Hb with SGNPs as the contrast agents.

Materials and Methods

Sample Preparation

Three blood samples with various Hb concentrations were selected to simulate the increased Hb concentration in the tumor area. The first sample was normal blood, the second had the Hb concentration of $\times 2$, and the third had the Hb concentration of $\times 4$ as normal blood.

The normal blood type was obtained from a healthy donor, whose blood cell test was confirmed by the hematology laboratory. To prepare the serum Hb concentrations of $\times 2$ and $\times 4$, centrifugation procedures were performed, and the blood samples were diluted with phosphate buffered saline (PBS).

Synthesis of spherical gold nanoparticles

Gold NPs were prepared through the Turkevich process by reducing the chloroauric acid (HAuCl_4).

After dissolving the HAuCl_4 , the solution was stirred rapidly, and the reducing agent was added simultaneously. As a result, the Au^{3+} ions were reduced to the Au^+ ions, and the disproportionate reaction occurred, while the three Au^+ ions provided the Au^{3+} and two AuO atoms. The AuO atoms acted as the center of nucleation, around which further Au^+ ions reduced.

In order to prevent the aggregation of the particles, a stabilizing agent that is attached to the nanoparticle surface is often added. After a few minutes, the color of the solution changes from light yellow to wine red. The method results in the AuNP diameter of 20 nanometers. In the Turkevich process for AuNP synthesis, citrate initially acts as the reducing agent and finally as the capping agent, stabilizing AuNP through the electrostatic interactions between the lone electron pairs on oxygen and the metal surface [23, 24]. Citrate ion concentration is the main influential factor in the shape, size, and reproducibility [25].

Synthesis of gold nanorods

In this study, a general two-step procedure was used to prepare the nanorods. In the first step (seed reaction), the seeds were formed by reducing HAuCl_4 with sodium borohydride. At the second stage (growth), the seeds were added to a solution, in which more HAuCl_4 was reduced by ascorbic acid. Surfactant hexadecyltrimethylammonium bromide (CTAB), which was present in the growth stage, directed the growth of the seeds along one axis to form the rods. The seed solutions were prepared by slowly mixing the reaction vial manually three times. The mixture turned into deep yellow, and ice-cold sodium borohydride was added. Afterwards, the mixture was swirled gently for two minutes in order to initiate the reduction of gold. The solution immediately turned into murky brown and preserved at the constant temperature of 37°C for two hours prior to use.

The growth solutions were prepared by adding silver nitrate to CTAB and slowly inverting the reaction vial manually three times. Following that, HAuCl_4 was added to the mixture, and the mixture was inverted three times again. The solution turned into deep yellow color within a minute of mixing. After the subsequent addition of ascorbic acid, the mixture was swirled manually until it became colorless. The produced seed solution was added to this solution, which was swirled again so as to promote dispersion. The solution was stored

at the temperature of 28°C during the nanorod growth. The color of the solution turned into light pink within two hours [26].

Instrumentation

The average diameter and zeta potential were measured using the laser-scattering technique (Zetasizer Nano ZS90, Malvern Instruments, and Malvern, UK). Transmission electron microscopy (TEM) was conducted using a Philips CM10 microscope (Phillips, Eindhoven, the Netherlands) at the accelerating voltage of 100 kV.

After preparing the NPs and blood samples with three Hb concentrations, the gold NPs were combined with the blood samples. The ratio of the NPs in the blood was 1:100, which was considered to be a safe volume for the blood cell complex.

Breast phantom

The breast phantom used in the present study contained a major and a minor vessel with the diameters of 10 and five millimeters, respectively. These vessels had various heights from the base, representing the diverse vascular network distribution in the breast.

The phantom was composed of polyethylene ($[\text{C}_2\text{H}_4]_n\text{H}_2$). Due to the hydrogen-carbon chains in polyethylene, it is able to simulate the breast tissue. The most important reason for the use of this phantom was the differences in the vascular networks between healthy and cancerous breasts. Approximately 6 and 3.5 milliliters of each substance were injected into the major and minor vessels of the phantom, respectively. Details of the phantom are explained in [27].

Optical instrumentation

A near-infrared (NIR) light source from LEDs and a source at the wavelength of 635 ± 5 nanometers on a continuous wave mode were used. The Phwee 45 LED (Daneshyakhte Company, Iran) was also applied with the dimensions of $13.5\times 13.5\times 13$ mm³, as well as 50-watt power as the NIR source. The transmitted NIR light intensity values were measured using an optical power meter (model: PM100D, ThorLabs GmbH, Dachau, Germany).

The set-up of the experiment was performed using a power supply, collimator, phantom, and power meter. The distance between the source and phantom was estimated at six centimeters. Blood with various Hb concentrations with and without NPs was injected into the minor and

major vessels separately.

After the blood injection, the phantom was placed above the NIR source with a collimator (power supply: 18 V and 1100 mA). In this experiment, differences in the passing intensity (DPI) of the NIR from the Hb in the major and minor vessels in the breast phantom were measured using the following formula (1):

$$DPI\% = (PI \text{ without substance} - PI \text{ with substance}) / PI \text{ without substance} \times 100 \quad (1)$$

Where PI is the passing intensity of the light, DPI% was calculated by measuring the PI with and without NPs in similar and fixed points on the phantom in the middle of the vessel and one centimeter above its middle. DPI% represents the percentage of the difference in the transmitting intensity of the phantom with or without the NPs injected into the blood vessels. It is notable that the formula was used for both types of the SGNPs.

Statistical analysis

The intensity of the passing NIR was measured twice at each point on the phantom. The experiments were performed in triplicate, and the average of the three obtained values was considered as the intensity of the passing light.

Data analysis was performed in SPSS version 16.0 and R statistical software. Comparison of the groups in terms of the PI was carried out using t-test and Wilcoxon test. Data were expressed as mean and standard deviation, and a P-value of less than 0.05 was considered significant.

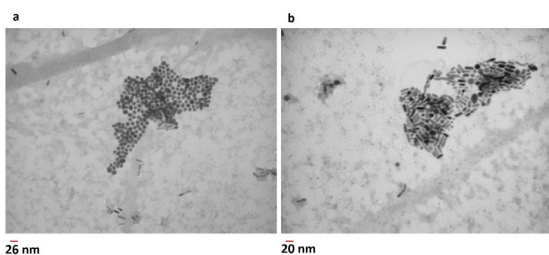


Fig 1. TEM Images of synthesized nanoparticles; a) Spherical gold nanoparticles, b) Gold nanorods

RESULTS

Fig 1 depicts the morphological analysis of the SGNPs and GNRs. The surface morphology of the SGNPs and GNRs was characterized using TEM. The TEM images of the SGNPs showed a rounded, spherical shape with the diameter of less than 20 nanometers. As for the GNRs, small particles were observed with a long cylindrical shape with the approximate length of 40 nanometers and

diameter of two nanometers.

Dynamic light scattering (DLS) and zeta potentials are depicted in Table 1. The size of the particles and zeta potential of the SGNPs and GNRs were investigated via DLS. The diameter of the SGNPs was estimated at 18 nanometers, while the diameter of the GNRs was approximately 40 nanometers.

Zeta potential analysis is often used to confirm the surface charge and stability of NPs in a solution. In the present study, the zeta potential analysis revealed that both SGNPs and GNRs had positive charges. As can be seen in Table 1, the zeta potential of the SGNPs was approximately 12 mV, while it was estimated to be 70 mV for GNRs based on CTAB due to the presence of a bilayer of CTAB on the surface of the GNRs.

Table 1. DLS and zeta potential analysis of gold nanoparticles; a1 and b1 are zeta potential and size of SGNPs; a2 and b2 are zeta potential and size of GNRs, respectively

	Size	Zeta potential
GNP	18.78	+12.2
GNR	44.45	+70.6

NIR passing ratio in the major and minor vessels without NPs

The PI values were calculated in the major vessels of the breast of the normal and cancerous blood types. In normal breast, the PI value was estimated to be 6.71 μw. However, when measured in cancerous breast, the value diminished to 5.59 and 3.97 μw at the x2 and x4 Hb concentrations, respectively. According to the obtained results, the PI values were directly dependent on the Hb concentration variations. Moreover, the PI values without NPs were assessed in the minor vessels. The PI values were calculated to be 5.55, 4.65, and 3.22 μw in normal blood and at the Hb concentrations of x2, and x4, respectively.

Table 2. Measurement of passing light intensity (PI) in water, normal blood, and hemoglobin (Hb) concentrations of x2 and x4 in major vessels with and without SGNPs

	Water	x1 Hb	x2 Hb	x4 Hb
PI without SGNPs	0.51±9.34	0.073±6.71	0.081±5.59	0.063±3.97
PI with SGNPs	0.083±7.45	0.085±3.62	0.1±2.24	0.081±1.64
PIRNR%	20.23	46.05	59.74	58.69
P-value	0.028	0.027	0.028	0.007

NIR passing ratio of SGNPs in major and minor vessels

After injecting various concentrations of Hb and SGNPs into the major vessel of the phantom,

the PI values of the normal breast changed to 3.62 μ w. In case of the cancerous breast cells, the PI values at the Hb concentrations of $\times 2$ and $\times 4$ were estimated at 2.40 and 1.64 μ w, respectively.

The differences in the PI values with and without the NPs of the normal blood and blood containing $\times 2$, and $\times 4$ Hb concentrations were calculated to be 46.05%, 57.06%, and 58.69%, respectively. The differences between the samples with and without the NPs were considered significant ($P < 0.05$) the results of DPI% measurement are presented in Table 2. Addition of the SGNPs to various Hb concentrations and injection into the minor vessels were associated with PI values of 2.97, 1.97, and 1.62 μ w in the normal blood and blood containing $\times 2$ and $\times 4$ Hb concentrations, respectively. The results of DPI% measurement are presented in Table 3. According to the information in this table, there were significant differences between Hb concentrations of $\times 1$, $\times 2$ ($P < 0.05$), and $\times 4$ ($P < 0.001$) in terms of the PI values of the samples with and without SGNPs.

Table3. Measurement of PI intensity in water, normal blood, and $\times 2$ and $\times 4$ Hb concentrations in minor vessels with and without SGNPs

	Water	$\times 1$ Hb	$\times 2$ Hb	$\times 4$ Hb
PI without SGNPs	0.83 \pm 7.25	0.099 \pm 5.55	0.087 \pm 4.65	0.067 \pm 3.22
PI with SGNPs	0.11 \pm 4.58	0.085 \pm 2.97	0.083 \pm 1.97	0.12 \pm 1.62
PIRNIIR%	36.82	46.68	56.08	49.68
P-value	0.018	0.027	0.012	0.007

NIR passing ratio of GNRS in major and minor vessels

When GNRs were injected into the major vessel with various Hb concentrations, the PI values were estimated to be 3.42, 2.13, and 1.98 μ w in both normal blood and blood containing $\times 2$ and $\times 4$ Hb concentrations, respectively. The variations in the PI intensity between the states with and without the GNRs are shown in Table 4. According to the information in this Table, there were significant differences between the cases with and without the GNRs ($P < 0.05$).

Table4. Measurement of passing light intensity in water, normal blood, and Hb concentrations of $\times 2$ and $\times 4$ in major vessels with and without GNRs

	Water	$\times 1$ Hb	$\times 2$ Hb	$\times 4$ Hb
PI without GNRs	0.070 \pm 9.26	0.12 \pm 6.81	0.097 \pm 5.61	0.11 \pm 4.03
PI with GNRs	0.069 \pm 6.72	0.12 \pm 3.42	0.11 \pm 2.13	0.097 \pm 1.98
DPI%	27.21	49.77	62.09	50.86
P-value	0.027	0.008	0.012	0.018

Comparison of the $\times 2$ and $\times 4$ Hb concentrations with the normal breast between SGNPs and GNRs indicated a significant difference in terms of the PI values between the Hb concentrations of $\times 2$

($P < 0.05$), $\times 4$ ($P < 0.05$), and $\times 1$.

After in the injection of various Hb concentrations and the GNRs into the minor vessel of the phantom, the PI and DPI% values were measured, and the results are shown in Table 5. According to the information in this table, there were significant differences in terms of the PI values between the Hb concentrations of $\times 1$, $\times 2$ ($P < 0.05$), and $\times 4$ ($P < 0.001$) in the cases with and without GNRs.

Table 5. Measurement of Passing Light Intensity in Water, Normal Blood, and Hb Concentrations of $\times 2$ and $\times 4$ in Minor Vessels with and without GNRs

	Water	$\times 1$ Hb	$\times 2$ Hb	$\times 4$ Hb
PI without GNRs	0.97 \pm 7.34	0.10 \pm 5.45	0.10 \pm 4.620	0.12 \pm 3.23
PI with GNRs	0.11 \pm 3.78	0.11 \pm 2.29	0.098 \pm 1.50	0.21 \pm 1.29
DPI%	48.50	57.03	67.53	60.06
P-value	0.027	0.017	0.015	0.007

Comparison of various vessel sizes and their effects on light transmission with GNRs and SGNPs indicated significant differences between the normal blood and blood containing $\times 2$ and $\times 4$ Hb concentrations. The details on the comparison of the NPs and vessel sizes are depicted in Fig 2.

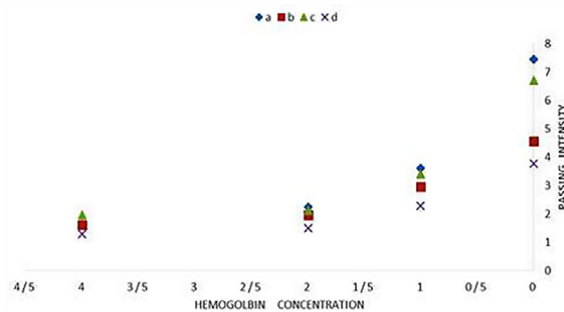


Fig 2. Comparison of passing light in major and minor vessels with SGNPs and GNRs; a) SGNPs in major vessel; b) SGNPs in minor vessel; c) GNRs in major vessel; d) GNRs in minor vessel

DISCUSSION

According to the results of the present study, the addition of NPs to various concentrations of Hb could be a practical method to determine vascular contrasts. The PI of the NIR in the major and minor vessels of the breast phantom indicated different variations with and without GNRs and SGNPs. Therefore, it could be concluded that GNRs and SGNPs could be used as vascular contrast media for the early diagnosis of breast cancer.

According to the findings of the current research, the PI values were significantly different in normal blood and the blood containing the Hb concentrations of $\times 2$ and $\times 4$. Furthermore, the DPI% values for the Hb concentrations of

×1, ×2, and ×4 were positively correlated with the increased Hb concentration. This difference became more significant with the addition of the GNRs and SGNPs. GNRs have a higher surface-to-volume ratio, which increases the reactivity and absorption of these NPs [12, 14]. Another study has also indicated that the shape of SGNPs could influence the interfacial properties in typical aquatic conditions [17].

According to the measurements in the present study, SGNPs could change the light intensity when passing Hb through the absorption and scattering of the NIR light. In both minor and major vessels, the intensity of light transmission decreased with the increased Hb concentration. Changes in the light intensity in the major and minor vessels were considered significant without the NPs. In addition, use of the NPs was associated with better contrast in minor vessels compared to major vessels with and without the NPs using the NIR optical method.

According to the results of the present study, the Hb concentration of ×2 was associated with a more significant difference between the presence and absence of the SGNPs. Our measurements also indicated that at Hb concentrations of ×2 and ×4 acted as Hb simulation in pre- and post-menopausal women, which is considered to be a beneficial finding in both these populations.

NIR imaging is a non-ionizing method recommended for every age group. This assay is economical as well. Gold NPs are considered to be safe materials for biological applications, which can be injected without definitive health problems. Furthermore, synthesis of both rod-shaped and spherical NPs are simple and economical. According to the results of the present study, SGNPs and GNRs could distinguish breast cancer blood from healthy blood in the early stages of formation. Furthermore, it is recommended that NIR optical imaging be employed for the prescreening of breast cancer owing to its non-invasiveness and potential for early diagnosis.

In a previous study, with Hb concentrations of ×2 and ×4 without NPs in the major vessel, the mean NIR transmissions were reported to be 5.38 and 6.66 μw , respectively [27]. However, the results of the present study showed that with SGNPs, these values were 2.24 and 1.64 μw , while they were 2.13 and 1.98 μw with GNRs at the Hb concentrations of ×2 and ×4, respectively. The difference between the experiments carried out with SGNPs was approximately 58% at ×2 Hb

concentration and 75% at ×4 Hb concentrations. In addition, the difference with GNRs was estimated to be 60% (×2 Hb concentration) and 70% (×4 Hb concentration). In the mentioned study, the measurement of the absorption and scattering per micron properties of the gold NPs also indicated that the magnitude of the gold nanorods was higher compared to nanoshells and nanospheres [14].

In another research, with Hb concentrations of ×2 and ×4 in the major vessel, the mean NIR transmissions by spectrometry was reported to be 8.56 and 8.33 μw , respectively [20]. The difference between the mentioned study and the current research in case of SGNPs was approximately 73% at Hb concentration of ×2 and 80% at Hb concentration of ×4. Moreover, the difference in case of GNRs was 75% (×2 Hb concentration) and 76.23% (×4 Hb concentration).

CONCLUSION

According to the results, SGNPs and GNRs in normal and cancerous breast induce differences in the transmission intensity of the NIR through Hb concentrations. Furthermore, the vascular contrast developed by the GNRs was observed to be higher compared to the use of SGNPs. Therefore, it could be concluded that The NIR light in combination with gold NPs has the potential for the early diagnosis of breast cancer.

ACKNOWLEDGMENTS

This work was supported by the office of the vice president for research in Tabriz University of Medical Sciences, Iran.

REFERENCES

1. Siegel RL, Miller KD, Jemal A. Cancer statistics. *CA*. 2015; 65(1): 5-29.
2. Gautherie M. Thermopathology of breast cancer: measurement and analysis of in vivo temperature and blood flow. *Ann NY AcadSci*. 1980; 335(1): 383-415.
3. Mehnati P, Tirtash MJ. Comparative efficacy of four imaging instruments for breast cancer screening. *APJCP*. 2015; 16(15): 67-86.
4. Warner E, Plewes D, Shumak R, Catzavelos G, Di Prospero L, Yaffe M. Comparison of breast magnetic resonance imaging, mammography, and ultrasound for surveillance of women at high risk for hereditary breast cancer. *JCO*. 2001; 19(15): 3524-3531.
5. Simick MK, Jong RA, Wilson BC, Lilge LD. Non-ionizing near-infrared radiation transillumination spectroscopy for breast tissue density and assessment of breast cancer risk. *JBO*. 2004; 9(4): 794-804.
6. Thomlinson R. Changes of oxygenation in tumours in relation

- to irradiation. The Relationship of Time and Dose in the Radiation Therapy of Cancer. Karger Publishers.1969; 3:p. 109-121.
7. Weidner N, Folkman J, Pozza F, Bevilacqua P, Allred EN, Moore DH. Tumor angiogenesis: a new significant and independent prognostic indicator in early-stage breast carcinoma. JNCI. 1992; 84(24): 15-87.
 8. Anderson PG, Kainerstorfer JM, Sassaroli A, Krishnamurthy N, Homer MJ, Graham RA. Broadband optical mammography: chromophore concentration and hemoglobin saturation contrast in breast cancer. PLOS one. 2015; 10(3): 117-322.
 9. Spinelli L, Torricelli A, Pifferi A, Taroni P, Danesini G, Cubeddu R. Characterization of female breast lesions from multi-wavelength time-resolved optical mammography. Phys med and biol. 2005; 50(11): 24-89.
 10. van de Ven S, Elias S, Wiethoff A, van der Voort M, Leproux A, Nielsen T. Diffuse optical tomography of the breast: initial validation in benign cysts. Mol Imaging Biol. 2009; 64(2): 11-70.
 11. Leff DR, Warren OJ, Enfield LC, Gibson A, Athanasiou T, Patten DK. Diffuse optical imaging of the healthy and diseased breast: a systematic review. Breast Cancer Res Treat. 2008; 108(1): 9-22.
 12. Srivastava A, Yadav R, Rai V, Ganguly T, Deb S, editors. Surface plasmon resonance in gold nanoparticles. AIP Conference Proceedings; AIP(2012).
 13. Daraee H, Eatemadi A, Abbasi E, Fekri Aval S, Kouhi M, Akbarzadeh A. Application of gold nanoparticles in biomedical and drug delivery. Artific cell Nanomed and biotech. 2016; 44(1): 4-22.
 14. Jain PK, Lee KS, El-Sayed IH, El-Sayed MA. Calculated absorption and scattering properties of gold nanoparticles of different size, shape, and composition: applications in biological imaging and biomedicine. JCP B. 2006; 110(14): 38-48.
 15. Huang X, Jain PK, El-Sayed IH, El-Sayed MA. Gold nanoparticles: interesting optical properties and recent applications in cancer diagnostics and therapy. NLM. 2007; 2(5): 68-93.
 16. Giljohann DA, Seferos DS, Daniel WL, Massich MD, Patel PC, Mirkin CA. AngewChemInt Ed Engl. 2010; 49(19): 80-94.
 17. Afrooz AN, Sivalapalan ST, Murphy CJ, Hussain SM, Schlager JJ, Saleh NB. Spheres vs. rods: "The shape of gold nanoparticles influences aggregation and deposition behavior. JO Chemosphere. 2013; 91(1): 82-98.
 18. El-Brolosy T, Abdallah T, Mohamed MB, Abdallah S, Easawi K, Negm S. Shape and size dependence of the surface plasmon resonance of gold nanoparticles studied by Photoacoustic technique. EPJ. 2008; 153(1): 361-413.
 19. Ntziachristos V, Bremer C, Weissleder R. Fluorescence imaging with near-infrared light: new technological advances that enable in vivo molecular imaging. Europe radiol. 2003; 13(1): 195-208.
 20. Mehnati P, Tirtash MJ, Zakerhamidi MS, Mehnati P. Assessing Absorption Coefficient of Hemoglobin in the Breast Phantom Using Near-Infrared Spectroscopy. IRAN J RADIOL. 2016; 13(4): 154-167.
 21. Taroni P, Pifferi A, Torricelli A, Spinelli L, Danesini G, Cubeddu R. Do shorter wavelengths improve contrast in optical mammography. Physics in Medic & Biolo. 2004; 49(7): 120-132
 22. Kosaka N, Ogawa M, Choyke PL, Kobayashi H. Clinical implications of near-infrared fluorescence imaging in cancer. Futu Oncol. 2006; 5(9): 150-168.
 23. Herizchi R, Abbasi E, Milani M, Akbarzadeh A. Current methods for synthesis of gold nanoparticles. Artific cell Nanomed and biotech. 2016; 44(2): 596-602.
 24. Reddy VR. "Gold nanoparticles: synthesis and applications .Synlett. 2006; 2006(11): 179_211.
 25. Chugh H, Sood D, Chandra I, Tomar V, Dhawan G, Chandra R. "Role of gold and silver nanoparticles in cancer nanomedicine. Artific cell Nanomed and biotech. 2018; 29(2): 1-23
 26. Gole A, Murphy CJ. Seed-mediated synthesis of gold nanorods: role of the size and nature of the seed. CM. 2004; 16(19): 36-40.
 27. Mehnati P, Khorram S, Zakerhamidi MS, Fahima F. Near-Infrared Visual Differentiation in Normal and Abnormal Breast Using Hemoglobin Concentrations. JLMS. 2018; 9(1): 50-57.